



TITLE:

Phase-locking of octave-spanning optical frequency comb based on Kerr-lens mode-locked Yb:KYW laser to reference laser

AUTHOR(S):

Mitaki, Masatoshi; Sugiyama, Kazuhiko

CITATION:

Mitaki, Masatoshi ...[et al]. Phase-locking of octave-spanning optical frequency comb based on Kerr-lens mode-locked Yb:KYW laser to reference laser. Japanese Journal of Applied Physics 2021, 60(2): 022003.

ISSUE DATE:

2021-01-19

URL:

<http://hdl.handle.net/2433/263823>

RIGHT:

This is an author-created, un-copyedited version of an article accepted for publication in Japanese Journal of Applied Physics. The publisher is not responsible for any errors or omissions in this version of the manuscript or any version derived from it. The Version of Record is available online at <https://doi.org/10.35848/1347-4065/abd86c>; The full-text file will be made open to the public on 19 January 2022 in accordance with publisher's "Terms and Conditions for Self-Archiving"; This is not the published version. Please cite only the published version. この論文は出版社版ではありません。引用の際には出版社版をご確認ください。

Phase-locking of octave-spanning optical frequency comb based on Kerr-lens mode-locked Yb:KYW laser to reference laser

Masatoshi Mitaki¹ and Kazuhiko Sugiyama^{1*}

¹*Graduate School of Electric Science and Engineering, Kyoto University, Katsura, Nishikyo, Kyoto 615-8510, Japan*

We phase locked an octave-spanning optical frequency comb based on a laser-diode-pumped Kerr-lens mode-locked Yb:KYW laser to a reference laser. We controlled the cavity length of the mode-locked laser to phase lock the mode frequency of the comb to the reference laser. This was conducted using a fast piezoelectric-actuated mirror on a lead-filled mount, which was aimed at damping the mechanical resonances. We achieved a servo bandwidth of 200 kHz, a residual phase noise of 0.47 rad, and a power concentration to a carrier of 91 %. To extend the locking duration of the carrier-envelope offset frequency, we compensated its slow drift using the position of the Yb:KYW crystal while the pump-laser power was controlled to achieve its phase locking. We continuously maintained the full phase locking of the comb for 3 h until the reference lasers were out of lock.

1. Introduction

An octave-spanning optical frequency comb (OFC) has been an inevitable tool in optical frequency metrology since optical frequency measurements were first demonstrated with respect to microwave frequency standards.¹⁻³⁾ Stabilization of the OFCs to the reference lasers was subsequently realized.^{4,5)} This enables us to evaluate the reproducibility of optical frequency standards, called optical clocks, because the uncertainties of such clocks are superior to those of microwave frequency standards and reach approximately 10^{-18} ,⁶⁻⁸⁾ whereas the uncertainty of the OFC was proved to be better than 10^{-19} .⁹⁾ Comparison between optical clocks referenced to different transitions has an application to exploring a temporal variation of the fine structure constant.¹⁰⁻¹²⁾ Furthermore, an OFC phase locked to an optical reference generates an ultra-low noise and a stable radiofrequency (RF) or microwave frequency.^{13, 14)}

In the applications indicated above, a tight phase locking of a residual phase noise smaller than $\pm\pi/2$ to the reference laser is required to prevent a degradation of its frequency stability. A long continuous operation is inevitable to realize an optical frequency comparison at their uncertainties and to use the generated RF or microwave frequency as a reference in other

*E-mail: sugiyama.kazuhiko.5r@kyoto-u.ac.jp

measurements.

The tight phase locking of an OFC to a reference laser requires fast transducers to control the mode frequency of the OFC. Intracavity electro-optic modulators (EOM) have been introduced in OFCs based on mode-locked fiber lasers.^{15,16)} Although the phase locking using the intracavity EOM was recently applied in an OFC based on a laser-diode-pumped solid-state laser,¹⁷⁾ the intracavity EOM requires attention to the optical damage and additional dispersion management. Extending the servo bandwidth of a piezoelectric-actuated mirror is another direction for improvement. The piezoelectric-actuated mirror is free from optical damage and the introduction of additional dispersion. A bandwidth of a few hundred kilohertz is realized using several inventions, i.e., damping mechanical resonances using a lead-filled mount¹⁸⁾ or a wedged aluminum-iron alloy plate,¹⁹⁾ and surrounding with soft elastic materials.²⁰⁾ We achieved a tight phase locking of the mode frequency of an OFC based on a mode-locked titanium-sapphire (Ti:sapphire) laser using a piezoelectric-actuated mirror on a lead-filled mount.²¹⁾

For a long continuous operation, OFCs based on mode-locked fiber lasers have been developed.^{22,23)} Although OFCs based on mode-locked fiber lasers had a relatively large phase noise at the early stage of development, new techniques have been invented to overcome this problem.²⁴⁾ Laser-diode (LD)-pumped mode-locked solid-state lasers can be an alternative to a fiber laser from the viewpoint of a low running cost. They even have the potential for a better substitution owing to a low noise intrinsically. We are developing an OFC based on a LD-pumped mode-locked ytterbium-doped potassium-yttrium-tungstate (Yb:KYW) laser.²⁵⁾ The Yb:KYW laser has additional advantages. We can use a reliable LD developed for erbium-doped fiber amplifiers owing to a pumping wavelength of 981 nm. A small quantum defect caused by the difference between the pumping and lasing wavelength of ~ 1030 nm results in low heat generation.

In this paper, we describe the phase locking of a LD-pumped Kerr-lens mode-locked Yb:KYW laser to a reference laser by controlling the mode frequency using a fast piezoelectric-actuated mirror on a lead-filled mount. We obtained a wider servo-bandwidth than that in our previous measurement,²¹⁾ and a better residual phase noise than that measured in a previous study on an OFC based on a mode-locked Yb:KYW laser.²⁶⁾

The mode frequency $f(n)$ of an OFC can be described as follows: $f(n) = n f_{\text{rep}} + f_{\text{CEO}}$, where f_{rep} is the pulse-repetition frequency, f_{CEO} is the carrier-envelope offset frequency, and n is the mode number. A full phase locking of the OFC simultaneously requires a phase locking of f_{CEO} . Owing to a large mode number of $\sim 10^5$, phase locking to a RF reference

is sufficient for f_{CEO} . In our previous study, we phase locked f_{CEO} by controlling only the pump-laser power, as a widely used approach.³⁾ In the case of a mode-locked Yb:KYW laser, the linewidth of f_{CEO} must be narrower than the response frequency of 45 kHz to the pump-laser power to phase lock f_{CEO} .²⁷⁾ We found that the pump-laser power not only controls the center frequency of f_{CEO} it also changes the linewidth of f_{CEO} .²⁵⁾ Therefore, a cancellation of the drift of f_{CEO} increases the f_{CEO} linewidth and finally renders f_{CEO} out of phase locking. We measured that the locking range of f_{CEO} , i.e., the range of the center frequency of f_{CEO} where the f_{CEO} linewidth is maintained at narrower than 45 kHz, was ~ 4 MHz when the position of the Yb:KYW crystal along the beam direction was controlled, and this locking range was 4 \sim 5 times larger than that when the pump-laser power was controlled.²⁵⁾ In this study, to improve the duration of continuous phase locking of f_{CEO} , we compensate a slow drift of f_{CEO} using the position of the Yb:KYW crystal. A summary including early stage of our experiments has been presented elsewhere.²⁸⁾

We describe the experimental setup in Sec. 2. We introduce the OFC developed in our previous work and describe two modifications to realize a tight phase locking to a reference laser for a lengthy period of time. In Sec. 3, we describe the results of the phase locking of the mode frequency of the OFC, and of the demonstration of the optical frequency comparison. In Sec. 4, we provide some concluding remarks regarding this study.

2. Experimental setup

The experimental setup is shown in Fig. 1. We modified our previously developed LD-pumped soft-aperture Kerr-lens mode-locked Yb:KYW laser.²⁵⁾ We summarize the performance common to the previous study as follows. The soft-aperture Kerr-lens mode-locking is realized at a transverse-mode regeneration observed around the center of the stability region of the laser cavity.^{29,30)} A 1-mm long 5 %-doped Yb:KYW crystal is lased. A mode-locked output power of 360 mW is generated from a single transverse-mode fiber-coupled LD of 750 mW as a pump laser (3S photonics, 1999CHP). The pulse-repetition rate, the center wavelength, the full width at half maximum (FWHM) of the spectrum, and the pulse duration are 91 MHz, 1030 nm, 8.0 nm, and 160 fs, respectively. We adjust the round-trip group delay dispersion (GDD) of the laser cavity using a combination of chirped mirrors to -7200 fs^2 to narrow the f_{CEO} linewidth. The Yb:KYW crystal is temperature-controlled using a thermo-electric cooler. The heatsink of the thermo-electric cooler is simply air-cooled owing to a low heat generation. The base plate of the laser cavity is temperature-controlled and the entire laser cavity is sealed in an aluminum box. These result in a continuous mode-locked oscillation

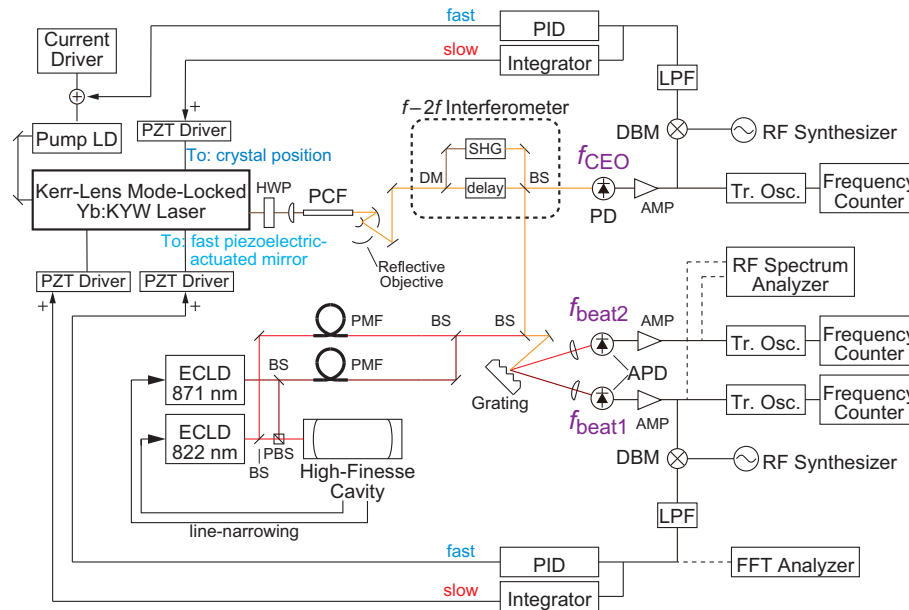


Fig. 1. Experimental setup. ECLD, extended-cavity laser diode; LD, laser diode; PCF, photonic-crystal fiber; PZT, piezoelectric transducer; PD, photo diode; APD, avalanche photo diode; AMP, amplifier; DBM, double-balanced mixer; LPF, low-pass filter; Tr. Osc., tracking oscillator; PID, proportional-integral-derivative controller; PMF, polarization-maintaining fiber; PBS, polarizing beam splitter; HWP, half-wave plate; DM, dichroic mirror; BS, 50:50 beam splitter.

that takes place for over a 1-month period without any adjustments.

The output from the mode-locked Yb:KYW laser is passed through a 50-mm long photonic-crystal fiber (PCF) with a core diameter of $3.3 \mu\text{m}$ (Blaze photonics, NL-3.3-890-02) to expand the spectrum by over one octave. We insert an optical isolator to eliminate the optical feedback, and a half-wave plate to adjust the spectral component in the output beam from the PCF for maximizing the signal-to-noise ratios (SNRs) of the beats with reference lasers and at f_{CEO} .

We detect the beat at f_{CEO} using an $f-2f$ interferometer.^{2,31)} We generate the second-harmonic of the OFC component at approximately 1200 nm using a 1-mm long $\beta - \text{BaB}_2\text{O}_4$ crystal. To phase lock f_{CEO} using the pump-laser power, a f_{CEO} linewidth is required to be narrower than the response frequency of 45 kHz.²⁷⁾ For this purpose, we adjust the bias pump-laser power and the Yb:KYW crystal position in addition to the round-trip cavity GDD.

We phase lock the f_{CEO} beat to a RF reference using the pump-laser power through an injection current of the pump LD. In our previous measurement, the following results were achieved: the SNR of a f_{CEO} beat of 40 dB with a resolution bandwidth (RBW) of 300 kHz under a free-running operation, a residual phase noise of 0.51 rad with an integration range of

1 Hz – 10 MHz, and the best locking duration of 2 h. The cavity length was controlled by the position of the translation stage using a stacked piezoelectric transducer (PZT) (NEC-Tokin AE0505D08) upon which one of the cavity-mirror mounts was placed. This was used for phase locking of f_{rep} to a RF reference in the previous measurement. In this study, this is used for compensation of a slow drift of the mode frequency phase locked to the reference laser to realize the phase locking of a long duration, owing to a large extension of the PZT.

We introduce two functions into the previous mode-locked Yb:KYW laser, i.e., a fast piezoelectric-actuated mirror and a position control of the Yb:KYW crystal. First, we replace the end mirror of the laser cavity with a fast piezoelectric-actuated mirror. This is aimed at a fast control of the cavity length to phase lock a mode of the OFC to a reference laser. The fast piezoelectric-actuated mirror has a lead-filled mount to damp the mechanical resonances of the PZT.¹⁸⁾ We glue a fast stacked PZT with a size of $5 \times 5 \times 2$ mm and a self-resonance frequency of 600 kHz (PI PL055.30) on the mount, and a low-dispersive quartz-substrate mirror with a diameter of 4 mm and a thickness of 1 mm on the PZT. We do not apply any weights during the gluing process to avoid damage to the thin mirror.

Second, we place a Yb:KYW crystal mount on an additional translation stage, the position of which is adjusted using a stacked PZT (NEC-Tokin AE0505D08). We still have no problem in the temperature control of the Yb:KYW crystal although the insertion of the additional translation stage reduces the size of the heatsink.

The optical reference frequency for phase locking of the OFC is provided by an extended-cavity laser diode (ECLD) having a wavelength of 871 nm line-narrowed to the resonance of a high-finesse Fabry-Perot cavity. Line-narrowing is conducted using an FM sideband technique.³²⁾ The high-finesse cavity is made of an ultralow-expansion (ULE) glass and has a finesse of 25,000. To demonstrate the optical frequency comparison, we use another ECLD having a wavelength of 822 nm line-narrowed to another resonance of the same high-finesse cavity used for line-narrowing the ECLD at 871 nm. The absolute linewidths of the two ECLDs are estimated to be < 500 Hz. The linewidth was previously measured from the beatnote between two independent line-narrowed ECLDs at 822 nm detected using a spectrum analyzer with a scanning time of 4 s for a 20 kHz span and from the spectra of the $^2S_{1/2} - ^2D_{3/2}$ transition at 435 nm in single $^{171}\text{Yb}^+$ ions.³³⁾

The two ECLDs are located on a different table from that where the OFC is placed. Each beam of the ECLD is independently transferred to the OFC table using polarization-maintaining optical fibers. The two beams are combined using a 50:50 beam splitter, and are then colinearly overlapped with the OFC beam using another 50:50 beam splitter. The

combined beams are dispersed using a diffraction grating. The beats between each ECLD frequency and a corresponding mode of the OFC are separately detected using an avalanche-photodiode.

The beat at 871 nm of the frequency f_{beat1} is amplified and is phase-sensitively detected using a double-balanced mixer (DBM) with a reference from a RF synthesizer to generate an error signal. The error signal through a proportional-integral-derivative (PID) controller is fed to a PZT controller to phase lock the beat at 871 nm to the reference, i.e., phase lock the mode frequency of the OFC to the ECLD at 871 nm. The error signal is analyzed using an FFT analyzer.

In the demonstration of optical frequency comparison, the mode frequency of the OFC is phase locked to the reference laser while f_{CEO} is simultaneously phase locked to another RF reference. We then measure the beat frequency f_{beat2} between another ECLD at a different wavelength of 822 nm and the other mode of the OFC. To monitor any cycle slips in the phase-locked loops (PLLs) for f_{beat1} and f_{CEO} , we simultaneously measure f_{beat1} and f_{CEO} in addition to f_{beat2} . The criterion for the cycle slip shows a frequency deviation of more than the inverse of the gate or average time of the frequency counter.³⁴⁾ To monitor the drift of the reference laser at 871 nm, we also measure f_{rep} . We operate a total of four frequency counters to measure f_{beat1} , f_{CEO} , f_{beat2} , and f_{rep} using the same trigger. The SNRs of the beats except for f_{rep} were marginal for a frequency measurement using the frequency counters without any miscounts.³⁵⁾ Therefore, we use tracking oscillators, i.e., voltage-controlled oscillators phase locked to the beats. All RF synthesizers and frequency counters reference a global-positioning-system (GPS) clock. In the specifications of the GPS clock, the relative stability at an averaging time of 1 s and the relative uncertainty by 1-day averaging are 1×10^{-11} and $\pm 2 \times 10^{-12}$, respectively.

3. Results

First, we phase locked f_{beat1} to the RF reference using the fast piezoelectric-actuated mirror. We obtained a SNR of 35 dB in the beat at f_{beat1} with a RBW of 300 kHz under a free running operation. The linewidth of the f_{beat1} spectrum was narrower than 30 kHz with a scanning time of 7 ms for a 10 MHz span of the RF spectrum analyzer, and increased to 1 MHz with a scanning time of over 57 ms owing to the acoustic noise of the mode-locked laser. When we closed the PLL and increased the servo gain, we observed a servo oscillation at 200 kHz. We set the corner frequencies based on the transitions from I to P and from P to D to 15 kHz and 250 kHz, respectively. The PI-corner frequency was adjusted to be fairly low. This indicates a

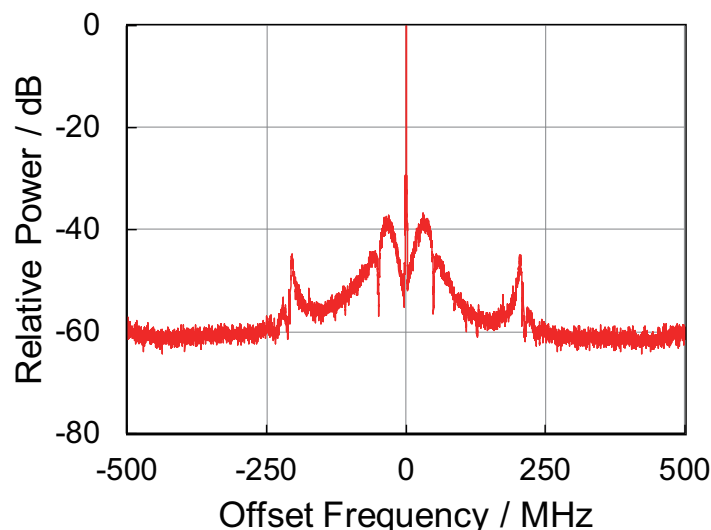


Fig. 2. Spectra of in-loop beat at f_{beat1} when PLL was closed. The resolution bandwidth (RBW) of the spectrum analyzer was 100 Hz.

phase lag of approximately 45 kHz. Figure 2 shows the beat spectrum at f_{beat1} when the PLL was closed. The power concentration to the carrier was 91 % within 1 MHz offset from the center frequency. We evaluated the residual phase noise from the phase noise power spectrum density measured from the error signal. The results are shown in Fig. 3. The residual phase noise was 0.47 rad from the integration of the power spectrum density of between 1 Hz and 10 MHz.

The servo-oscillation frequency was higher than that obtained in our previous study, i.e., 80 kHz, using an OFC based on a mode-locked Ti:sapphire laser.²¹⁾ This is caused by the use of a lighter mirror. The residual phase noise and the power concentration were better than those measured in a previous study using an OFC based on a mode-locked Yb:KYW laser, where the residual integrated phase noise was measured to be 0.4 rad by the integration between 0.1 Hz and 0.5 MHz.²⁶⁾ If we set the integration range to be between 1 Hz and 0.5 MHz, we estimate the residual phase noise to be 0.16 rad in our measurement. In this estimation, we suppose that the low-frequency components between 0.1 Hz and 1 Hz has little contribution to the residual phase noise. In addition, the sideband peak at approximately a 50 kHz-offset shown in Fig. 2 was -20 dB smaller than that detected in the previous study.²⁶⁾

Second, as a demonstration of the optical frequency comparison or optical frequency-ratio measurement, we measured the beat frequency with another ECLD at a different wavelength from that used for the phase locking while the modes of the OFC and f_{CEO} were simultaneously

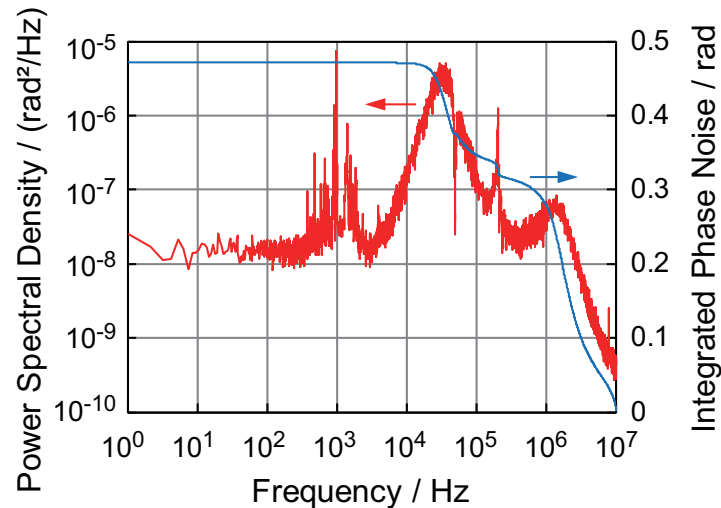


Fig. 3. Phase noise power spectral density analyzed from error signal in phase-locked loop for f_{beat1} and integrated phase noise of the in-loop beat at f_{beat1} . The error signal voltage was converted into the phase deviation using a constant ratio. The sinusoidal response of the mixer had a discrepancy from this linear approximation, but was only 2% at ± 0.5 rad.

phase locked. To conduct this measurement, we adjusted the output spectrum from the PCF using the half-wave plate placed before the input of the PCF to simultaneously optimize the SNRs of the three beats, i.e., f_{beat1} , f_{CEO} , and f_{beat2} . The SNRs of the beats at f_{beat1} , f_{CEO} , and f_{beat2} were 25, 35, and 20 dB, respectively, when the measurements were conducted.

We observed that the f_{CEO} linewidth was increased from 15 kHz at free running operation to more than 100 kHz when the PLL for f_{beat1} was closed, when it was detected using a spectrum analyzer with a scanning time of ~ 60 ms for a 1 MHz span. We measured that the extension of the fast PZT for phase locking of f_{beat1} changed the center frequency of f_{CEO} with a sensitivity of 14 MHz/ μm in addition to the mode frequency. The controlling voltage to the fast PZT from the PZT driver modulated the f_{CEO} according to the sensitivity. The dominant frequency component of the controlling voltage was lower than the instantaneous linewidth of the f_{beat1} spectrum at the free-running operation, which was narrower than 30 kHz as described above. This value was lower than the response bandwidth of f_{CEO} to the pump-laser power of 45 kHz. Therefore, we realized the simultaneous phase locking of f_{beat1} and f_{CEO} . The mechanism for the change of f_{CEO} by the extension of the fast PZT is not understood and further investigations are required.

Figures 4 (a, b) show the spectra of the in-loop beat at f_{beat1} , when the PLLs for f_{beat1} and f_{CEO} were closed. Although the SNR of f_{beat1} was decreased by 10 dB from the best

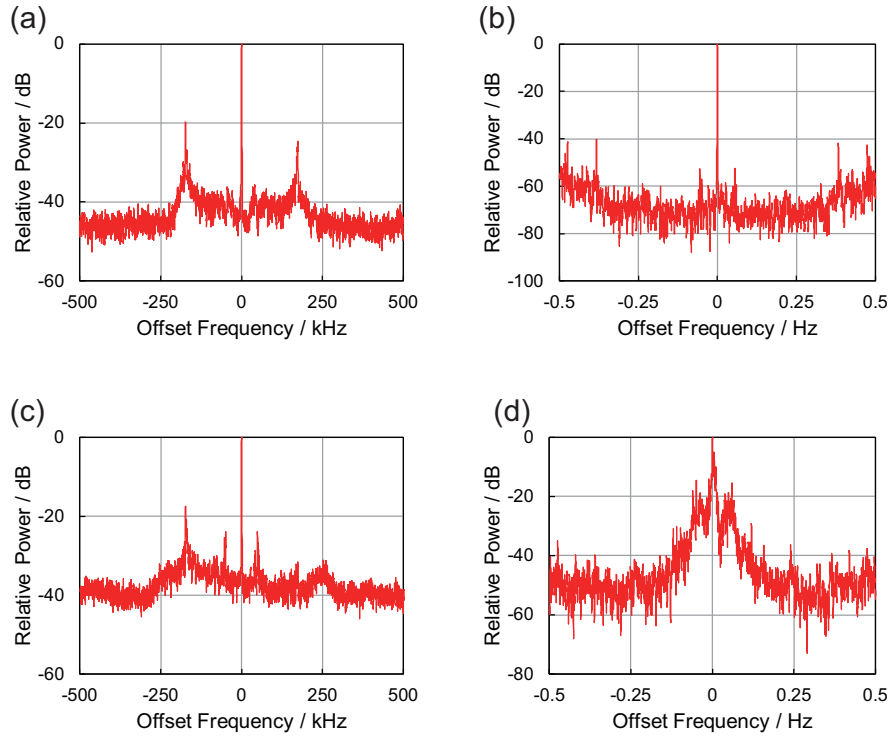


Fig. 4. Spectra of beat between a mode of the OFC and the reference lasers when PLLs for $f_{\text{beat}1}$ and f_{CEO} were closed. (a, b) in-loop beat note at $f_{\text{beat}1}$ at 871 nm and (c, d) out-of-loop beat note at $f_{\text{beat}2}$ at 822 nm. (a, c) 1-MHz span with a RBW of 1 kHz and (b, d) a 1-kHz span with a RBW of 1 Hz. We obtained these spectra at the servo gain just below the start of oscillation. Therefore, we sometimes observed sidebands at the servo oscillation frequency of ± 200 kHz and asymmetric spectra like (c).

SNR, which resulted in the in-loop beat spectrum shown in Fig. 2, we detected a carrier spectrum with a linewidth limited by the RBW of the RF spectrum analyzer, as shown in Fig. 4 (b). Figures 4 (c, d) show the spectra of the out-of-loop beat at $f_{\text{beat}2}$. From the spectrum of $f_{\text{beat}2}$ detected with a 1-MHz span, as shown in Fig. 4 (c), the spectral shape appeared to be transferred to the other modes of the comb because the two ECLDs were line-narrowed to the resonances of the same cavity, and the fluctuation of the cavity resonance was cancelled. However, when we detected the $f_{\text{beat}2}$ spectrum using a narrow RBW, we observed a residual linewidth and phase noises in the carrier spectrum as shown in Fig. 4 (d). Similar spectra were observed in our previous measurement using the OFC based on a mode-locked Ti:sapphire laser. We supposed that the residual linewidth and phase noises were caused by problems in the servo electronics for the line-narrowing of the reference lasers or the phase noise generation in the fibers used for beam transport.²¹⁾

The results of the simultaneous measurement of $f_{\text{beat}1}$, f_{CEO} , $f_{\text{beat}2}$, and f_{rep} are shown in Fig. 5. We continuously measured them for 3 h until one of the reference lasers was out of

lock with the resonance of the high-finesse cavity, despite having no help of the pre-scalers to extend the locking range in the PLLs for f_{beat1} and f_{CEO} . Note that the error signals and the controller outputs in the two PLLs for f_{beat1} and f_{CEO} did not reach $\pm\pi/2$ nor the maximum compensation, respectively. This indicates that the developed OFC has a potential for a longer continuous full phase-locked operation.

The cycle slips, which occurred in the 3-h phase locking were detected to be 0.24 % and 0.94 % for f_{beat1} and f_{CEO} , respectively, from a total of 10,692 measurements of an average time of 1 s. The cycle slips were sufficiently small. We discarded the measurement data of f_{beat2} and f_{rep} when the cycle slip was detected in the PLLs for f_{beat1} and f_{CEO} .

We observed a linear drift of $-15 \mu\text{Hz/s}$ in f_{rep} corresponding to -57Hz/s at 871 nm. This was caused by the drift of the resonance frequency of the high-finesse cavity in which the ECLD at 871 nm was line-narrowed because the temperature of the high-finesse cavity was not adjusted to that of the zero thermal expansion coefficient. Although this value was 4-16 times as large as the previous measurements,^{21,33)} it can be understood from a possible temperature change.

From the measurement results of f_{beat2} , the root Allan variance of the relative frequency of the ECLD at 822 nm to that at 871 nm was 3×10^{-14} at an averaging time of 1 s. The origin of the drift observed in f_{beat2} was not understood, because the two ECLDs were line-narrowed to the resonances of the same cavity and the temperature drifts of the resonances were cancelled, while a possible contribution from the mirror dispersion was estimated to be below the detectable level.²¹⁾ A similar drift was observed in our previous measurement using an octave-spanning OFC based on a mode-locked Ti:sapphire laser, and two possible origins of the drift were proposed: offset drifts in the controllers used for the line-narrowing, or Doppler shifts in the fibers used for a transfer of the beams of the reference lasers.²¹⁾ Further investigations are required for future improvements.

4. Conclusions

We realized the full phase locking of an OFC based on a LD-pumped Kerr-lens mode-locked Yb:KYW laser. The mode frequency was controlled using a fast piezoelectric-actuated mirror on a lead-filled mount with a servo bandwidth of 200 kHz. The residual phase noise was evaluated as 0.47 rad from the integration of the phase noise power spectrum density from 1 Hz to 10 MHz and the power concentration to the carrier of 91 % within a 1 MHz offset. To extend the locking duration of f_{CEO} , the drift of f_{CEO} was compensated using the position of the Yb:KYW crystal. We demonstrated an optical frequency comparison as we conducted the

measurement of the beat frequency between another mode of the phase-locked OFC and the second stabilized laser. We achieved a continuous measurement for 3 h. This measurement duration was limited by a locking of the reference laser, and the OFC developed showed the potential for a longer continuous operation.

Acknowledgment

We are grateful to Yasutaka Imai for operating the reference lasers. We would like to thank Masao Kitano for the support. This work was supported by the Support Center for Advanced Telecommunications Technology Research (SCAT); Innovative Techno-Hub for Integrated Medical Bio-imaging of the Project for Developing Innovation Systems, MEXT, Japan; Japan Society for the Promotion of Science (JSPS) (KAKENHI JP26287092).

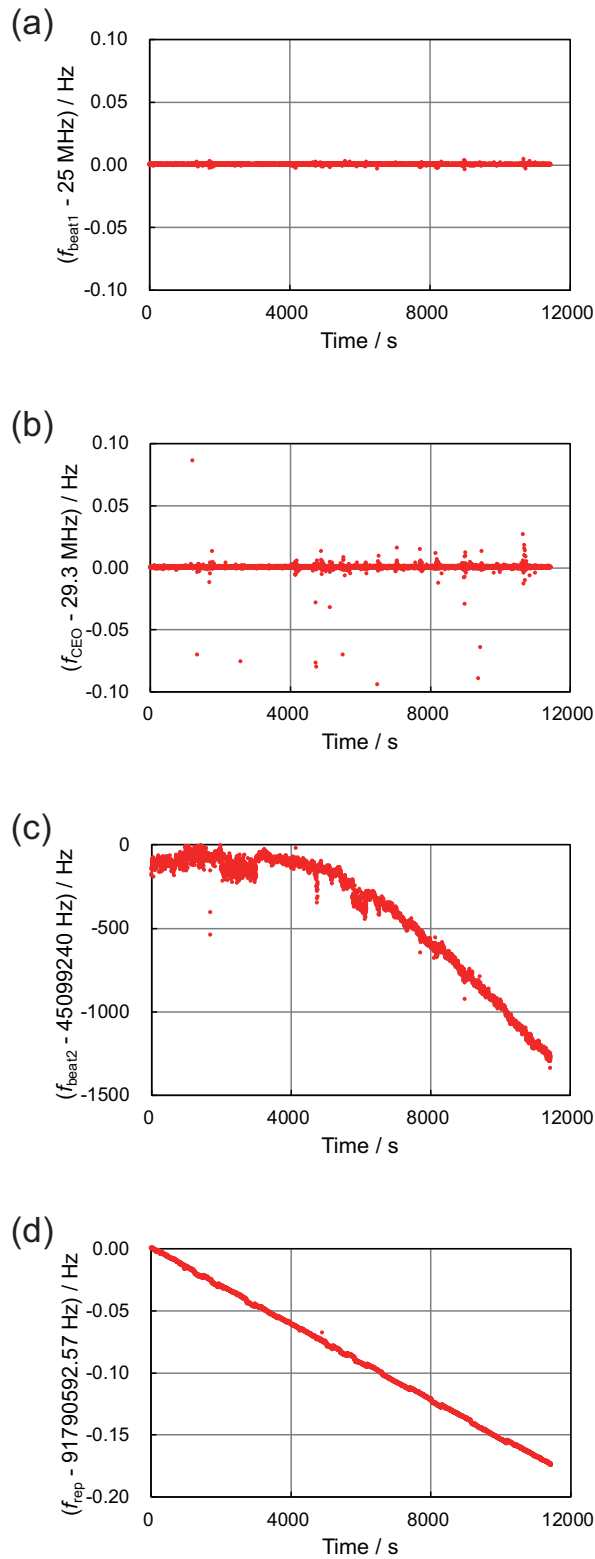


Fig. 5. Simultaneous frequency counting measurement of (a) f_{beat1} , (b) f_{CEO} , (c) f_{beat2} , and (d) f_{rep} in an average time τ_{gate} of 1 s with the same trigger. Here, f_{beat1} and f_{CEO} are the frequencies of the in-loop beat, and most of their fluctuations were much smaller than the criterion of the cycle slip of $1/\tau_{\text{gate}}$.

References

- 1) S. A. Diddams, D. J. Jones, J. Ye, S. T. Cundiff, J. L. Hall, J. K. Ranka, R. S. Windeler, R. Holzwarth, T. Udem, and T. W. Hänsch, *Phys. Rev. Lett.* **84**, 5102 (2000).
- 2) D. J. Jones, S. A. Diddams, J. K. Ranka, A. Stentz, R. S. Windeler, J. L. Hall, and S. T. Cundiff, *Science* **288**, 635 (2000).
- 3) R. Holzwarth, T. Udem, T. W. Hänsch, J. C. Knight, W. J. Wadsworth, and P. S. J. Russell, *Phys. Rev. Lett.* **85**, 2264 (2000).
- 4) S. A. Diddams, A. Bartels, T. M. Ramond, C. W. Oates, S. Bize, E. A. Curtis, J. C. Bergquist, and L. Hollberg, *IEEE J. Sel. Top. Quantum Electron.* **9**, 1072 (2003).
- 5) A. Bartels, C. W. Oates, L. Hollberg, and S. A. Diddams, *Opt. Lett.* **29**, 1081 (2004).
- 6) I. Ushijima, M. Takamoto, M. Das, T. Ohkubo, and H. Katori, *Nat. Photonics.* **9**, 185 (2015).
- 7) N. Huntemann, C. Sanner, B. Lipphardt, C. Tamm, and E. Peik, *Phys. Rev. Lett.* **116**, 063001 (2016).
- 8) S. M. Brewer, J.-S. Chen, E. R. Hankin, E. R. Clements, C.-W. Chou, D. J. Wineland, D. B. Hume, and D. R. Leibbrandt, *Phys. Rev. Lett.* **123**, 033201 (2019).
- 9) L.-S. Ma, Z. Bi, A. Bartels, L. Robertsson, M. Zucco, R. S. Windeler, G. Wilpers, C. Oates, L. Hollberg, and S. A. Diddams, *Science* **303**, 1843 (2004).
- 10) T. Rosenband, D. B. Hume, P. O. Schmidt, C. W. Chou, A. Brusch, L. Lorini, W. H. Oskay, R. E. Drullinger, T. M. Fortier, J. E. Stalnaker, S. A. Diddams, W. C. Swann, N. R. Newbury, W. M. Itano, D. J. Wineland, and J. C. Bergquist, *Science* **319**, 1808 (2008).
- 11) R. M. Godun, P. B. R. Nisbet-Jones, J. M. Jones, S. A. King, L. A. M. Johnson, H. S. Margolis, K. Szymaniec, S. N. Lea, K. Bongs, and P. Gill, *Phys. Rev. Lett.* **113**, 210801 (2014).
- 12) N. Huntemann, B. Lipphardt, C. Tamm, V. Gerginov, S. Weyers, and E. Peik, *Phys. Rev. Lett.* **113**, 210802 (2014).
- 13) T. M. Fortier, M. S. Kirchner, F. Quinlan, J. Taylor, J. C. Bergquist, T. Rosenband, N. Lemke, A. Ludlow, Y. Jiang, C. W. Oates, and S. A. Diddams, *Nat. Photonics* **5**, 425 (2011).
- 14) X. Xie, R. Bouchand, D. Nicolodi, M. Giunta, W. Hänsel, M. Lezius, A. Joshi, S. Datta, C. Alexandre, M. Lours, P.-A. Tremblin, G. Santarelli, R. Holzwarth, and Y. Le Coq, *Nat. Photonics* **11**, 44 (2017).

- 15) D. D. Hudson, K. W. Holman, R. J. Jones, S. T. Cundiff, J. Ye, and D. J. Jones, *Opt. Lett.* **30**, 2948 (2005).
- 16) Y. Nakajima, H. Inaba, K. Hosaka, K. Minoshima, A. Onae, M. Yasuda, T. Kohno, S. Kawato, T. Kobayashi, T. Katsuyama, and F.-L. Hong, *Opt. Express* **18**, 1667 (2010).
- 17) N. Torcheboeuf, G. Buchs, S. Kundermann, E. Portuondo-Campa, J. Bennès, and S. Lecomte, *Opt. Express* **25**, 2215 (2017).
- 18) T. C. Briles, D. C. Yost, A. Cingöz, J. Ye and T. R. Schibli, *Opt. Express* **18**, 9739 (2010).
- 19) T. Nakamura, S. Tani, I. Ito, M. Endo, and Y. Kobayashi, *Opt. Express* **28**, 16118 (2020).
- 20) D. Goldovsky, V. Jouravsky, and A. Pe'er, *Opt. Express* **24**, 28239 (2016).
- 21) S. Hatanaka, K. Sugiyama, M. Mitaki, M. Misono, S. N. Slyusarev, and M. Kitano, *Appl. Opt.* **56**, 3615 (2017).
- 22) F. Adler, K. Moutzouris, A. Leitenstorfer, H. Schnatz, B. Lipphardt, G. Grosche, and F. Tauser, *Opt. Express* **12**, 5872 (2004).
- 23) H. Inaba, Y. Daimon, F.-L. Hong, A. Onae, K. Minoshima, T. R. Schibli, H. Matsumoto, M. Hirano, T. Okuno, M. Onishi, and M. Nakazawa, *Opt. Express* **14**, 5223 (2006).
- 24) C. Benko, A. Ruehl, M. J. Martin, K. S. E. Eikema, M. E. Fermann, I. Hartl, and J. Ye, *Opt. Lett.* **37**, 2196 (2012).
- 25) M. Mitaki, K. Sugiyama, and M. Kitano, *Appl. Opt.* **57**, 5150 (2018).
- 26) S. A. Meyer, T. M. Fortier, S. Lecomte, and S. A. Diddams, *Appl. Phys. B* **112**, 565 (2013).
- 27) S. A. Meyer, J. A. Squier, and S. A. Diddams, *Eur. Phys. J. D.* **48**, 19 (2008).
- 28) M. Mitaki, K. Sugiyama, and M. Kitano, in *Advance Solid State Laser*, (Optical Society of America, 2016), paper JTu2A.26.
- 29) J.-H. Lin, M.-D. Wei, W.-F. Hsieh, and H.-H. Wu, *J. Opt. Soc. Am. B* **18**, 1069 (2001).
- 30) P. Wasylczyk and C. Radzewicz, *Laser Phys.* **19**, 129 (2009).
- 31) H. R. Telle, G. Steinmeyer, A. E. Dunlop, J. Stenger, D. H. Sutter, and U. Keller, *Appl. Phys. B* **69**, 327 (1999).
- 32) R. W. P. Drever, J. L. Hall, F. V. Kowalski, J. Hough, G. M. Ford, A. J. Munley, and H. Ward, *Appl. Phys. B* **31**, 97 (1983).
- 33) Y. Imai, T. Nishi, M. Nishizaki, S. Kawajiri, Y. Muroki, R. Ikuta, K. Matsumoto, M. Kitano, and K. Sugiyama, *Radio Sci.* **51**, 1385 (2016).
- 34) T. Udem, S. A. Diddams, K. R. Vogel, C. W. Oates, E. A. Curtis, W. D. Lee, W. M. Itano,

- R. E. Drullinger, J. C. Bergquist, and L. Hollberg, *Phys. Rev. Lett.* **86**, 4996 (2001).
- 35) K. Sugiyama, F.-L. Hong, J. Ishikawa, A. Onae, T. Ikegami, S. N. Slyusarev,
K. Minoshima, H. Matsumoto, H. Inaba, J. C. Knight, W. J. Wadsworth, and P. S. J.
Russell, *Jpn J. Appl. Phys.* **45**, 5051 (2006).